Polish Society of Composite Materials
Polskie Towarzystwo Materiałów Kompozytowych

24: 4 (2024) 213-219

COMPOSITES THEORY AND PRACTICE

ISSN (online): 2299-128X

Bartłomiej Przybyszewski[1,2]*, Rafał Kozera [1,2], Katarzyna Ziętkowska[1,2], Anna Labeda[1,2]
Christian W. Karl[3], Monika Pilz[4], Anna Boczkowska[1,2]

[1] *Technology Partners Foundation,ul. Bitwy Warszawskiej 1920 r. 7A, 02-366 Warsaw, Poland*
[2] *Warsaw University of Technology, Faculty of Materials Science and Engineering, ul. Woloska 141, 02-507 Warsaw, Poland*
[3] *SINTEF Industry, Department of Materials and Nanotechnology, Forskningsveien 1, 0373 Oslo, Norway*
[4] *SINTEF Industry, Department of Process Technology, Forskningsveien 1, 0373 Oslo, Norway*
**Corresponding author. E-mail: bartlomiej.przybyszewski.dokt@pw.edu.pl*

Received (Otrzymano) 29.03.2024

EFFECT OF UV LASER TEXTURIZATION ON HYDROPHOBIC AND ANTI-ICING PROPERTIES OF WATERBORNE POLYURETHANE NANOCOMPOSITE COATINGS

https://doi.org/10.62753/ctp.2024.01.4.4

Reducing ice buildup on different aerodynamic surfaces like airplane wings or wind turbine blades caused by the impact of supercooled water droplets can be achieved by creating surfaces featuring anti-icing capabilities. Hydrophobic surfaces are particularly promising due to their water-repelling attributes. In recent years, advancements in short-pulsed laser technologies have provided an efficient method for altering material surface properties. However, the effectiveness of such surfaces in preventing ice accumulation has yet to be validated. This study introduces a UV laser texturization approach for polymer surfaces. Laser patterning was employed to create periodic surface structures on the modified polyurethane coatings. The study investigated the influence of different laser parameters like pulse frequency, laser speed or pattern shape on the topographical features, hydrophobicity, and anti-icing properties of the resulting surfaces. Surface topography characterization was performed using scanning electron microscopy (SEM) and an optical profilometer. The wettability parameters, including the static contact angle and contact angle hysteresis, were measured to assess the impact of the wetting behavior and laser parameters on the materials under investigation. The anti-icing properties were evaluated by means of freezing delay time tests. The findings indicate that the laser texturization of waterborne polyurethane coatings enhances the hydrophobic and anti-icing properties of the investigated materials.

Keywords: hydrophobicity, anti-icing properties, waterborne polyurethane coatings, freezing delay time, laser texturization, UV laser patterning

INTRODUCTION

Durable and efficient surfaces and coatings with enhanced hydrophobicity and anti-icing properties have been a subject of substantial interest in various industrial sectors, including aerospace, automotive, and marine engineering [1-4]. Especially anti-icing coatings play a crucial role in aviation due to their ability to mitigate the risks associated with ice accumulation on the surfaces of planes, helicopters or unmanned aerial vehicles (UAVs) [5, 6]. In particular, such parts like engine inlets, the leading edges of wings or propellers or sensors are susceptible to icing [7, 8]. Ice accumulation on these structures poses significant safety hazards. It can disrupt aerodynamic performance, increase drag and affect the performance of measuring equipment, leading to potential accidents [9]. Moreover, ice accretion on aircraft requires substantial time and resources, including de-icing procedures, which cause flight delays, increase fuel consumption and disrupt airline schedules [10]. Novel coatings and surfaces with anti-icing properties offer significant support in the mitigation of ice formation, thereby improving operational efficiency, reducing maintenance downtime and enhancing aircraft reliability [11]. In addition, the utilization of anti-icing coatings can result in significant cost savings for airlines and operators. By reducing the frequency of de-icing procedures and minimizing the need for anti-icing fluids, icephobic coatings help lower operational expenses associated with aircraft maintenance and ground operations [12]. Improved aerodynamic performance and fuel efficiency contribute to long-term cost savings for airlines.

Surfaces and coatings with anti-icing properties offer enhanced performance in cold climates by minimizing ice accumulation and adhesion on surfaces, thus reducing the need for frequent de-icing procedures [13]. They typically contain low-surface-energy materials that make it difficult for ice to adhere. These coatings can be applied to a variety of substrates, including metals, polymers, and composites. Siloxane-based coatings and fluorinated polymers are commonly used

in icephobic coatings [14-16]. Hong et al. [17] developed a novel super-repellent icephobic coating. Polydimethylsiloxane (PDMS) and cross-linked poly[hexeafluorobisphenol A-co-cyclotriphosphazene] microspheres (PHC) were prepared by single-step precipitation polymerization without further surface modifications. The facilely fabricated coating demonstrated a high static water contact angle of ~164° and a low sliding angle of ~3.7°. More importantly, the coating exhibited exceptional mechanical durability against various types of damage owing to the synergistic effects of the micro/nanoscale surface structure in addition to the strong and stable interaction between the PHC particles and PDMS. More remarkably, the coating exhibited good self-cleaning and anti-icing properties in a damp environment (–15 °C).

In this work we investigated waterborne polyurethane coatings (WPU). They have emerged as a promising alternative to traditional solvent-based coatings because of their eco-friendly nature, low volatile organic compound (VOC) content, and excellent film-forming properties [18, 19]. These coatings offer superior adhesion, flexibility, and corrosion resistance, making them suitable for a wide range of applications [20, 21]. Moreover, the inherent tunability of polyurethane chemistry allows the incorporation of functional additives or modifiers to tailor specific properties, such as hydrophobicity and ice-repellency [22]. To induce hydrophobic properties and an anti-icing effect in polymer coatings, surface texturization via laser irradiation can be utilized. It is a promising technique due to its precision, versatility, and environmental friendliness. Unfortunately, in the state of the art only few works can be found on the topic of laser texturization of polyurethane coatings [23-25]. Estevam-Alves et al. [26] employed a UV laser to produce periodic surface structures on polyurethane substrates with spatial periods ranging from 0.5 μm to 5.0 μm. The influence of the laser energy density on the quality and topographical characteristics of the produced micropatterns was investigated. Unfortunately, only results of the basic properties (wettability) were presented. Neither the anti-icing properties, nor the durability of the produced surfaces were studied. In this paper, we present the hybrid modification of WPU coatings. Volumetric modification via the addition of organosilicon modifiers was followed by nanosecond UV laser surface texturing. The effect of the performed modifications on the hydrophobic, anti-icing properties and durability of the waterborne polyurethane coatings is presented.

MATERIALS AND METHODS

The material used in the present study was white Aerowave 5001 topcoat from AkzoNobel Aerospace Coatings (Netherlands). It is a water-based, 3-component isocyanate cured polyurethane finish for interior and exterior use. It was used in combination with Aerowave 2002 primer, also from AkzoNobel. 2024 aluminum alloy coupons were first cleaned in an ultrasonic acetone bath for 15 min. Initially, both the primer components were mixed according to the manufacturer's indications and applied as the first layer with subsequent application of the Aerowave 5001 polyurethane coating as the top coating layer by mixing according to the manufacturer's technical data sheet. Spray application of the Aerowave system was carried out on the Al alloy coupons by means of a Walther® Pilot XIII air spray gun (Germany) achieving an average dry layer thickness of 50 μm ±10 μm for the PU-coating (top layer). The primer layer was left to dry for 3 h before the polyurethane material was sprayed on as the top layer and left for 3 weeks at room temperature before surface texturization and testing were carried out. Prior to coating deposition, the WPU mixture was modified by an addition of 2 wt.% of an organosilicon-based additive. The synthesis and characterization of the used additive were extensively described in other works by the authors [27-29]. An Nd:YAG ultraviolet laser Matrix 355 from Coherent was employed to process the samples and manufacture patterns on the surface of the samples. The maximum average power of the laser was 5 W and wavelength 355 nm. The pulse duration was 10 ns. The pulse repetition frequency was changed from 20 kHz to 50 kHz, thus the energy per pulse changed from 250 μJ to 100 μJ. The galvanometer intelliSCAN 14 from SCANLAB was used to perform laser texturization. The linear laser beam speed was changed from 250 mm/s to 1000 mm/s. Two different patterns were produced: lines (L) and grid (G) (Fig. 1). The spacing between the line markings was constant and set at 60 μm.

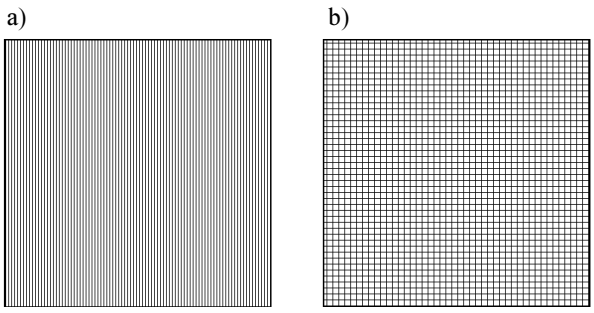

Fig. 1. Patterns manufactured on samples: a) parallel lines, b) grid

The laser processing parameters of the investigated samples are presented in Table 1.

In order to assess effect of the performed texturization on surface development, the topography of the coatings was examined. Surface roughness measurements were carried out by means of an S Lynx SensoSCAN 6 non-contact light profilometer from Sensofar, using the interferometry lens with 20x magnification. All the measurements were acquired from a 840 μm x 840 μm area. Three different randomly selected areas were measured on each sample. The R_a and R_z roughness parameters were determined.

TABLE 1. **Laser processing parameters**

Processing type no.	Speed [mm/s]	Pulse frequency [kHz]	Energy per pulse [µJ]
1	250	20	250
2		30	167
3		40	125
4		50	100
5	500	20	250
6		30	167
7		40	125
8		50	100
9	750	20	250
10		30	167
11		40	125
12		50	100
13	1000	20	250
14		30	167
15		40	125
16		50	100

Microscopic observations of the laser patterns were carried out utilizing a Hitachi TM-3000 SEM. Specimens 1 cm x 1 cm were cut from the manufactured plates, glued to the microscope stage using carbon tape and transferred to the microscope chamber. To increase the electrical conductivity of the specimens, they were coated with a conductive layer employing a sputtering machine SC7640 from Polaron equipped with an Au-Pd target.

In order to assess the effect of the performed modifications on the hydrophobic properties of the polyurethane coatings, surface wettability measurements were carried out using a DataPhysics OCA 15 goniometer with the sessile drop method. For measurements of the static contact angle (SCA) a 5-µl deionized water droplet was deposited on the test surface and a photo was taken. The contact angle hysteresis was measured by the inflating/deflating method with the needle-in mode. The standard deviation for each measurement was ±1°. The wettability parameters were measured before and after the frosting/defrosting durability test.

Freezing delay time measurements were carried out by means of the OCA 15 goniometer from DataPhysics, and a cooling chamber. The tests were conducted according to the methodology proposed in paper [30].

Icing/de-icing cycles were performed to assess the durability of the investigated coatings and examine their hydrophobic behavior after exposure to such harsh conditions. The tests were performed in an MK115 climatic chamber from Binder. The samples were cooled to –20 °C and held at this temperature for 30 min. Next, the temperature was set at 25 °C, and after reaching it the samples were kept for 30 min as well. Such a procedure was repeated 500 times. After that, the wettability parameters were measured.

RESULTS AND DISCUSSION

Scanning electron microscopy

SEM analyses were conducted to assess the effectiveness of the laser patterning parameters in relation to the actual condition of the treated specimens. Measurements of the line thickness and spacing distance were performed, as outlined in Table 2. The resulting micrographs of exemplary specimens are presented in Figure 2. Additionally, each micrograph features a droplet image taken during the wettability tests. Further details are provided in section below.

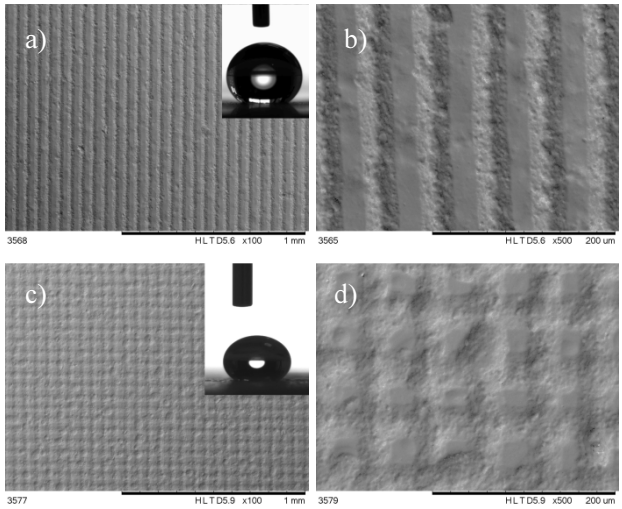

Fig. 2. SEM micrographs of specimens after laser processing. Laser processing type no. 4: a) lines, 100x, b) lines, 500x, c) grid, 100x, d) 500x

TABLE 2. **Texture parameters measured from SEM micrographs**

Processing type no.	Pattern	Spacing distance [µm]	Line thickness [µm]	Pattern	Spacing distance [µm]	Line thickness [µm]
1	Lines	61.2	31.2	Grid	62.3	32.5
2		63.8	33.5		61.5	33.1
3		59.7	32.9		60.7	32.2
4		62.7	34.1		59.9	30.5
5		60.8	31.2		60.4	29.6
6		62.6	30.9		63.5	31.9
7		61.5	33.4		62.8	32.1
8		59.9	32.0		61.2	31.6
9		60.3	31.1		60.6	31.9
10		64.2	32.2		58.9	30.4
11		58.6	29.8		61.0	30.6
12		62.8	31.1		60.7	31.0
13		62.2	32.5		59.4	33.3
14		59.6	33.1		60.2	31.5
15		64.2	32.8		61.8	30.8
16		61.2	31.7		63.1	31.5

It can be seen both from the micrographs and values taken from Table 2 that for both patterns (lines and grid) and all the sample processing types, the geometry

of the obtained patterns are similar. The quality of the manufactured lines is high, they are uniform, parallel and the edges are sharp. Comparing the spacing distance values from Table 2 and the distance assumed during pattern manufacturing (60 µm), it can be seen that these values are similar, regardless of the type of pattern; the distances measured on the SEM micrographs are almost equal, similar to those set in the laser parameters. The line thickness is slightly higher for the lower laser speeds and higher pulse frequencies. Observing the micrographs displayed in Figure 2, it is evident that the laser texturization was successful, demonstrating controlled ablation of the coating material. Distinct patterns are discernible, and the measured spacings closely align with the applied laser parameters.

Optical profilometry

In Table 3, the surface roughness parameters of the manufactured samples are shown. Analyzing the obtained values, it is visible that the laser patterning increased the roughness parameters, i.e. the R_a value of the untreated sample is 0.2 µm, whereas the lowest value for a sample after laser processing is 1.09 µm and the highest is 5.95 µm. Out of the samples with the linear pattern, the one with processing type no. 13 achieved the lowest roughness (R_a 1.09 µm, R_z 4.32 µm). The highest values were obtained by the sample with processing type no. 4. Similar values were received for the grid pattern. The maximum roughness values were observed for processing type no. 4 (R_a 5.95 µm, R_z 21.66 µm), while the lowest were observed for type no. 13 (R_a 1.18 µm, R_z 6.02 µm). It can be concluded that the roughness of the linear pattern is slightly lower than that of the grid pattern. In addition, it is easy to see that roughness increases with decreasing laser speed. Moreover, for each laser speed, the higher the pulse frequency, the higher the surface roughness. The values of the roughness parameters were compared with the 3D profiles of the manufactured patterns on the samples (Fig. 3). The presented profilograms are representative of each laser processing type.

TABLE 3. **Roughness parameter values for samples after laser treatment**

Processing type no.	Pattern	R_a [µm]	R_z [µm]	Pattern	R_a [µm]	R_z [µm]
none	-	0.2	0.12	-	-	-
1	Lines	1.53	8.49	Grid	1.68	9.59
2		2.35	12.17		3.25	14.08
3		3.48	17.44		4.56	17.52
4		4.65	21.04		5.95	21.66
5		1.39	9.87		1.72	9.14
6		1.45	10.11		1.98	10.26
7		1.51	10.75		2.2	11.40
8		1.81	11.14		3.02	13.98
9		1.22	6.55		1.35	7.92
10		1.36	6.92		1.48	8.56
11		1.39	7.45		1.63	10.45
12		1.43	7.67		1.65	11.31
13		1.09	4.32		1.18	6.02
14		1.14	5.12		1.26	7.13
15		1.26	5.70		1.45	7.85
16		1.35	6.16		1.59	9.03

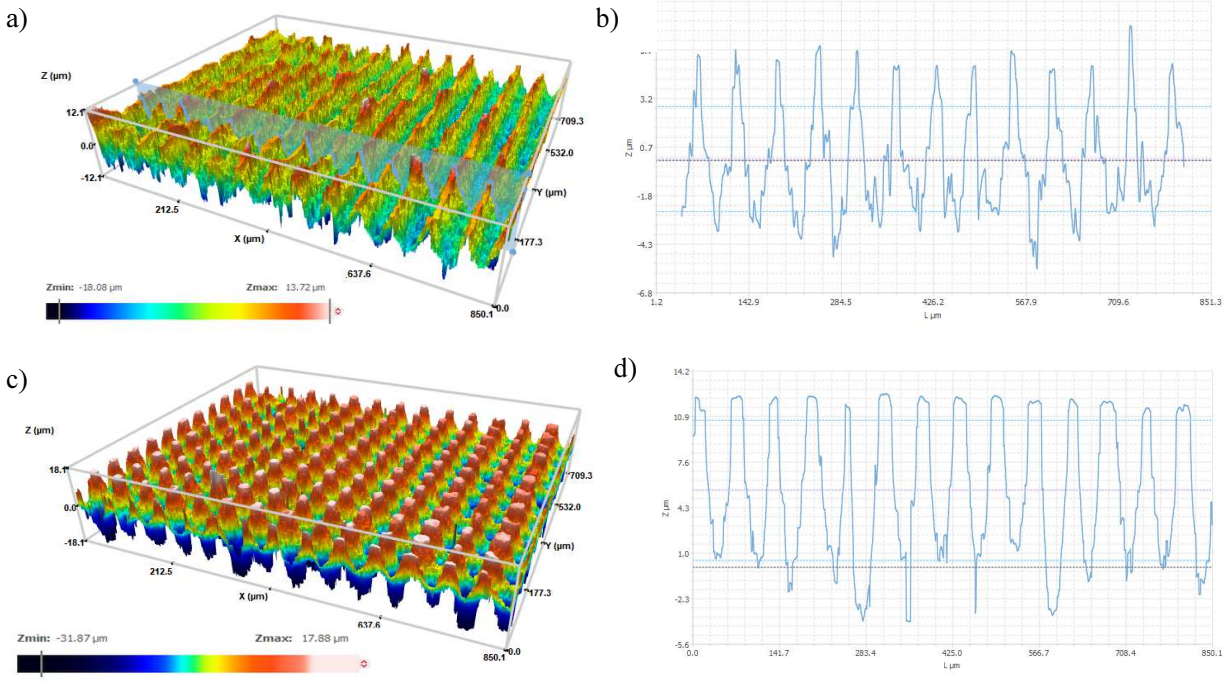

Fig. 3. Representative profilogram of sample after laser texturization. Laser processing type no. 4: a) lines, 3D scan, b) lines, 2D profile, c) grid, 3D scan, b) grid, 2D profile

Based on the 3D and 2D profiles obtained from the profilometer, as illustrated in Figure 3, it can be confirmed that the profiles align consistently with the SEM micrographs. The patterns exhibit regularity, featuring periodic distances between the peaks, and uniform peak widths. Furthermore, the obtained surfaces indicate a well-controlled patterning process. The peaks observed in Figure 3 are regular and uniform. In the case of the grid pattern, it is likely that points where the lines intersect are deeper processed than the whole lines. In a few cases, the profiles reveal minor imperfections in the overall shape, yet no significant disruptions in the manufactured patterns or deviations from the pattern geometry are observed.

Wettability

The assessment of sample wettability relied on determining the contact angle and contact angle hysteresis values, detailed in Table 4. Additionally, images depicting the droplets on the textured surfaces were presented in Figure 2.

TABLE 4. **Wettability parameters of investigated samples**

Processing type no.	Pattern	SCA [°]	CAH [°]	Pattern	SCA [°]	CAH [°]
none	-	91	45	-	-	-
1	Lines	131	17	Grid	129	16
2		135	15		130	13
3		134	18		139	11
4		140	12		141	9
5		130	22		123	25
6		135	20		137	13
7		135	18		140	10
8		137	14		140	8
9		120	33		117	36
10		131	25		133	28
11		132	28		134	25
12		133	24		136	25
13		104	40		116	34
14		121	38		128	26
15		130	23		132	22
16		132	25		136	19

The reference coating (without laser treatment) exhibited a static contact angle of 91°, thus demonstrating a degree of hydrophobic behavior. However, it straddles the boundary between hydrophilicity and hydrophobicity. It becomes evident that the implementation of laser patterning enhances the hydrophobicity of the surfaces. Among the samples with the linear pattern, processing types no. 4 and 8 yield the most favorable results, with measured contact angles ranging between 137° and 140°. The lowest increases in contact angle were noticed for processing types no. 9 and 13. In the case of the grid pattern, the highest contact angle values were recorded for processing types 4, 7 and 8, while the lowest were for 9 and 13. The contact angle hysteresis is the lowest for processing type number 4 (12° and 9°) and 8 (14° and 8°), for the linear and grid patterns, respectively. The highest values were obtained for processing type 13 (lines) and 9 (grid), 40° and 36°, respectively. Overall, the values for all the texturized specimens are lower than for the sample before laser treatment. It can be assumed that, in general, the higher the pulse frequency, the higher the hydrophobic properties (high SCA, low CAH). Moreover, highest hydrophobic properties were obtained for the 250 mm/s and 500 mm/s laser speeds. In the case of the higher scanning speed, the hydrophobic properties began to decrease.

Freezing delay time

Because of the long duration of the freezing delay time test, it was carried out only on selected samples, with the highest wettability parameters. The results for the reference and treated samples are shown in Table 5.

TABLE 5. **Results of freezing delay time tests compared with contact angle**

Processing type no.	Pattern	FDT [min]	SCA [°]	Pattern	FDT [min]	SCA [°]
none	-	6	91	-	-	-
4	Lines	192	140	Grid	211	141
7		102	135		145	140
8		110	137		156	140

Laser texturization of the coatings increased the freezing time, as the reference sample achieved only 6 min. The values obtained for the linear pattern are longer than for non-texturized coating, reaching the maximum time of 192 min for processing type no. 4. The freezing delay time of samples with the grid pattern is significantly extended, as the maximum value exceeds 200 min (Processing no. 4). In Table 5 the SCA values are also presented for correlation analysis. It can be noticed that the longest FDT was observed for the surfaces with the highest contact angles.

Frosting/de-frosting cycling

As was mentioned above, hydrophobic and anti-icing coatings easily lose their superior properties after exposure to harsh environments, especially after frosting/de-frosting cycles. This type of durability test is particularly important as it simulates the real conditions of operating infrastructures like airplane wings or wind turbine blades. Moreover, this test distinctly verifies the hydrophobic as well as icephobic properties of the manufactured coatings/surfaces. In this paper the changes in the wettability parameters (SCA) of selected samples after 500 icing/de-icing cycles are presented in Table 6.

TABLE 6. **Results of static contact angle for selected samples before and after frosting/de-frosting test**

Processing type no.	Pattern	SCA [°]	SCA after [°]	Pattern	SCA [°]	SCA after [°]
none	-	91	78	-	-	-
4	Lines	140	139	Grid	141	139
7		135	133		140	137
8		137	136		140	138

It can be observed that the contact angle of non-texturized sample decreased from 91° to 78° after 500 cycles. For the samples after laser texturization, only a slight decrease (1-2°) was observed. It can be stated that the samples after laser texturization exhibited stable hydrophobic properties after exposure to harsh conditions (frosting/de-frosting).

SUMMARY AND CONCLUSIONS

In this paper the effect of laser texturization on the functional properties of waterborne polyurethane coatings was presented. Different laser parameters were tested and their influence on the quality, roughness and hydrophobic properties of the manufactured samples was assessed. It was noticed that the pulse frequency and laser speed do not significantly affect the geometry of the produced patterns. The spacing distance and line width for each processing type were similar to each other and consistent with the assumptions. Nevertheless, it was observed that the laser processing parameters significantly influenced the surface roughness. It was observed that the surface roughness values increased with lower laser speed and higher pulse frequency. The highest R_a and R_z parameters were observed for processing type no. 4, where the laser speed was 250 mm/s and pulse frequency 50 kHz. Moreover, the surface roughness was slightly higher for the surfaces with the grid pattern. It was proved that the performed laser texturization significantly increases the hydrophobic properties. The wettability parameters of the polyurethane coatings increased from 90° to 140°, likely as a result of changes in the contact area of water droplets with the investigated surface. This also influenced the freezing delay time of the samples. For selected samples it was proved that laser texturization resulted in a drastic increase in FDT, from 6 to more than 200 minutes. Good stability of the hydrophobic properties was confirmed in the durability tests. Further research is planned to analyze the correlations between the hydrophobic and anti-icing properties in more detail.

Acknowledgments

This work was financially supported by the National Centre for Research and Development in the framework of Polish Norwegian Grants, project "Anti-icing sustainable solutions for the development and application of icephobic coatings" No. NOR/POLNOR/IceMan/0061/2019.

REFERENCES

[1] Zeng Q., Zhou H., Huang J., Guo Z., Review on the recent development of durable superhydrophobic materials for practical applications, Nanoscale 2021, 13(27), 11734--11764, DOI: 10.1039/D1NR01936H.

[2] Momen G., Jafari R., Farzaneh M., Ice repellency behaviour of superhydrophobic surfaces: Effects of atmospheric icing conditions and surface roughness, Appl. Surf. Sci., 2015, 349, 211-218, DOI: 10.1016/J.APSUSC.2015.04.180.

[3] Wang Y., Zhang J., Dodiuk H. et al., The reduction in ice adhesion using controlled topography superhydrophobic coatings, J. Coatings Technol. Res., Published online 2022, October, 18, 1-15, DOI: 10.1007/S11998-022-00682-2/METRICS.

[4] Bai Y., Zhang H., Shao Y., Zhang H., Zhu J., Recent progresses of superhydrophobic coatings in different application fields: An overview, Coatings 2021, 11(2), 116, DOI: 10.3390/COATINGS11020116.

[5] Cao Y., Tan W., Wu Z., Aircraft icing: An ongoing threat to aviation safety, Aerosp. Sci. Technol. 2018, 75, 353-385, DOI: 10.1016/J.AST.2017.12.028.

[6] Caliskan F., Hajiyev C., A review of in-flight detection and identification of aircraft icing and reconfigurable control, Prog. Aerosp. Sci. 2013, 60, 12-34, DOI: 10.1016/J.PAEROSCI.2012.11.001.

[7] Rasmussen R., Wade C., Hage F. et al., New ground deicing hazard associated with freezing drizzle ingestion by jet engines, J. Aircr. 2006, 43(5), 1448-1457, DOI: 10.2514/1.20799.

[8] Su Q., Chang S., Zhao Y., Zheng H., Dang C., A review of loop heat pipes for aircraft anti-icing applications, Appl. Therm. Eng. 2018, 130, 528-540, DOI: 10.1016/J.APPLTHERMALENG.2017.11.030.

[9] Cao Y., Wu Z., Su Y., Xu Z., Aircraft flight characteristics in icing conditions, Prog. Aerosp. Sci. 2015, 74, 62-80, DOI: 10.1016/J.PAEROSCI.2014.12.001

[10] Yang T., Gao F., Bozhko S., Wheeler P., Power Electronic Systems for Aircraft, In: Control of Power Electronic Convertes and Systems, Vol. 2, Published online 2018, January 1, 333-368, DOI: 10.1016/B978-0-12-816136-4.00025-7.

[11] Huttunen-Saarivirta E., Kuokkala V.T., Kokkonen J., Paajanen H., Corrosion effects of runway de-icing chemicals on aircraft alloys and coatings, Mater. Chem. Phys. 2011, 126(1-2), 138-151, DOI: 10.1016/j.matchemphys.2010.11.049.

[12] Antonini C., Innocenti M., Horn T., Marengo M., Amirfazli A., Understanding the effect of superhydrophobic coatings on energy reduction in anti-icing systems, Cold. Reg. Sci. Technol. 2011, 67(1-2), 58-67, DOI: 10.1016/J.COLDREGIONS.2011.02.006.

[13] Zheng H., Liu G., Nienhaus B.B., Buddingh J.V., Ice-shedding polymer coatings with high hardness but low ice adhesion, ACS Appl. Mater. Interfaces 2022, 14(4), 6071--6082. DOI: 10.1021/ACSAMI.1C23483/SUPPL_FILE/AM1C23483_SI_007.MP4.

[14] Brassard J.D., Sarkar D.K., Perron J., Fluorine based superhydrophobic coatings, Appl. Sci. 2012, 2(2), 453-464, DOI: 10.3390/APP2020453.

[15] Li H., Li X., Luo C., Zhao Y., Yuan X., Icephobicity of polydimethylsiloxane-b-poly(fluorinated acrylate), Thin Solid Films 2014, 573, 67-73, DOI: 10.1016/j.tsf.2014.11.007.

[16] Bogdanowicz K.A., Dutkiewicz M., Maciejewski H. et al., Siloxane resins as hydrophobic self-cleaning layers for silicon and dye-sensitized solar cells: material and application aspects, RSC Adv. 2022, 12(30), 19154-19170, DOI: 10.1039/D2RA02698H.

[17] Hong S., Wang R., Huang X., Liu H., Facile one-step fabrication of PHC/PDMS anti-icing coatings with mechanical properties and good durability, Prog. Org. Coat. 2019, 135, 263-269, DOI: 10.1016/J.PORGCOAT.2019.06.016.

[18] Song Y., Zhai R., Zhang J. et al., Effect of fluorine atom positions on the properties of waterborne polyurethanes, Prog. Org. Coat. 2024, 189, 108330, DOI: 10.1016/J.PORGCOAT.2024.108330.

[19] Zhang J., Jiang Z., Wang Y. et al., Abrasion resistant waterborne polyurethane coatings based on dual crosslinked structure, Prog. Org. Coat. 2024, 190, 108336, DOI: 10.1016/J.PORGCOAT.2024.108336.

[20] Zhang Z., Han X., Jia L., Yu W., Zheng Q., Highly water-resistant transparent waterborne polyurethane thermal-insulation coating material with multiple self-crosslinking network based on controllably activated end-capping reagent, Prog. Org. Coat. 2024, 187, 108104, DOI: 10.1016/J.PORGCOAT.2023.108104.

[21] Li G., Tan Y., Li Z. et al., Advances in waterborne polyurethane matting resins: A review, Appl. Surf. Sci. Adv. 2024, 19, 100557, DOI: 10.1016/J.APSADV.2023.100557.

[22] Lee D., Park J., Woo M.J. et al., Impact of polymer structure in polyurethane topcoats on anti-icing properties, Appl. Surf. Sci. 2024, 667, 160402, DOI: 10.1016/J.APSUSC.2024.160402

[23] Zhang Y., Li X., Lu L., Guan Y., Anti-icing polyurethane coating on glass fiber-reinforced plastics induced by femtosecond laser texturing, Appl. Surf. Sci. 2024, 662, 160077, DOI: 10.1016/J.APSUSC.2024.160077.

[24] Pola J., Thermal reactive modifications of polymer surfaces by infrared laser radiation, J. Anal. Appl. Pyrolysis 2023, 169, 105819, DOI: 10.1016/J.JAAP.2022.105819.

[25] Martinez-Calderon M., Haase T.A., Novikova N.I. et al., Turning industrial paints superhydrophobic via femtosecond laser surface hierarchical structuring, Prog. Org. Coat. 2022, 163, 106625, DOI: 10.1016/J.PORGCOAT.2021.106625.

[26] Estevam-Alves R., Günther D., Dani S. et al., UV direct laser interference patterning of polyurethane substrates as tool for tuning its surface wettability, Appl. Surf. Sci. 2016, 374, 222-228, DOI: 10.1016/j.apsusc.2015.11.119.

[27] Kozera R., Ziętkowska K., Przybyszewski B. et al., The effect of modification of gelcoat based on unsaturated polyester resin with polysiloxanes on icephobicity, hydrophobicity and durability, Colloids Surfaces A Physicochem. Eng. Asp. 2023, 675, 132025, DOI: 10.1016/J.COLSURFA.2023.132025.

[28] Kozera R., Ziętkowska K., Przybyszewski B. et al., Spherosilicate-modified epoxy coatings with enhanced icephobic properties for wind turbines applications, Colloids Surfaces A Physicochem. Eng. Asp. 2023, 679, 132475, DOI: 10.1016/J.COLSURFA.2023.132475.

[29] Kozera R., Ziętkowska K., Krawczyk Z. et al., Modification of gelcoat based unsaturated polyester resin with functionalized octaspherosilicates to reduce the ice adhesion strength, Colloids Surfaces A Physicochem. Eng. Asp. 2024, 688, 133549, DOI: 10.1016/J.COLSURFA.2024.133549.

[30] Kozera R., Przybyszewski B., Krawczyk Z.D. et al., Hydrophobic and anti-icing behavior of uv-laser-treated polyester resin-based gelcoats, Processes 2020, 8(12), 1-19, DOI: 10.3390/pr8121642.